A thin-film silicon/silicon hetero-junction hybrid solar cell for photoelectrochemical water-reduction applications

Vasudevan, Ravi; Thanawala, Z; Han, Lihao; Buijs, Thom; Tan, Hairen; Deligiannis, Dimitris; Perez Rodriguez, Paula; Digdaya, Ibadillah; Smith, Wilson; Zeman, Miro

DOI
10.1016/j.solmat.2016.02.006

Publication date
2016

Document Version
Publisher's PDF, also known as Version of record

Published in
Solar Energy Materials & Solar Cells

Solar Energy Materials & Solar Cells 150 (2016) 82–87

Contents lists available at ScienceDirect

Solar Energy Materials & Solar Cells

journal homepage: www.elsevier.com/locate/solmat

A thin-film silicon/silicon hetero-junction hybrid solar cell for photoelectrochemical water-reduction applications

Ravi Vasudevan [a,*], Zaid Thanawala [a], Lihao Han [a], Thom Buijs [a], Hairen Tan [a], Dimitrios Deligiannis [a], Paula Perez-Rodriguez [a], Ibadillah A. Digdaya [b], Wilson A. Smith [b], Miro Zeman [a], Arno H.M. Smets [a]

[a] Photovoltaic Materials and Devices (PVMD) Laboratory, Department of Electrical Sustainable Energy, Delft University of Technology, P.O. Box 5031, Delft 2600GA, The Netherlands
[b] Materials for Energy Conversion and Storage (MECS), Department of Chemical Engineering, Delft University of Technology, P.O. Box 5045, Delft 2600GA, The Netherlands

ARTICLE INFO

Article history:
Received 25 August 2015
Received in revised form
2 November 2015
Accepted 11 February 2016
Available online 2 March 2016

Keywords:
Silicon heterojunction
Thin-film silicon
Tandem
Hybrid
Water-splitting
Silicon

ABSTRACT

A hybrid tandem solar cell consisting of a thin-film, nanocrystalline silicon top junction and a silicon heterojunction bottom junction is proposed as a supporting solar cell for photoelectrochemical applications. Tunneling recombination junction engineering is shown to be an important consideration in designing this type of solar cell. The best hybrid cell produced has a spectral utilization of 30.6 mA cm^{-2} a J_{SC} of 14 mA cm^{-2}, a V_{OC} of 1.1 V, a fill factor of 0.67 and thus an efficiency of 10.3%. A high solar-to-hydrogen efficiency of 7.9% can be predicted when using the hybrid cell in conjunction with current a-SiC photocathode technology.

1. Introduction

Photoelectrochemical (PEC) water splitting is becoming a viable and important method for solar energy conversion in the form of hydrogen fuels. A complete PEC cell requires two electrodes where one of them is photoactive (either a photocathode or photoanode) and the other electrode is called the counterelectrode. Solar-to-hydrogen (STH) conversion efficiencies of up to 18.3% have been reported [1]. However, these devices use expensive, scarce materials such as gallium arsenide and gallium indium phosphide, which are also not highly water-resistant [1,2]. Thin-film amorphous silicon carbide (a-SiC:H) has been used as a photocathode material for water reduction as it is a much more practical material for larger scale applications [3–6]. This technology is showing a lot of promise as a photocathode based on a-$Si_{0.9}C_{0.1}$:H can theoretically generate a maximum photocurrent density of 15 mA cm^{-2} or a STH efficiency of 18% corresponding to its bandgap of 2.0 eV [7,8]. Fig. 1 illustrates the fundamental components of an a-SiC:H based photocathode consisting of a thin intrinsic a-SiC:H absorber as well as a gradient doped boron-doped a-SiC:H (p) layer and a phosphorous doped nanocrystalline silicon oxide (nc-SiO_x) layer.

A challenge to achieving a high STH efficiency is that the low photovoltage of photocathodes (0.8 V in the case of a-SiC:H technology) is not enough to overcome the thermodynamic water-splitting potential of 1.23 V [9]. In addition to this 1.23 V the overpotentials necessary to drive the overall redox reactions need to be considered [10]. As a result, an external bias is required for this structure to achieve its maximum current density [4].

Integrating a solar cell at the back of the PEC device to realize a monolithic PEC/PV device can directly produce hydrogen without any external bias [11–13]. Various PEC/PV configurations have been demonstrated based on amorphous silicon alloys, such as a-SiC:H/a-Si:H, a-SiC:H/a-Si:H/nc-Si:H, and a-SiC:H/nc-Si:H/nc-Si:H junctions [8]. The STH efficiency in all of these cases is primarily hindered by the potential current density of the supporting solar cell based on thin-film silicon technology.

For typical lab-scale PV device engineering, the target is usually to achieve the highest solar-to-electricity (STE) efficiency under an AM 1.5 spectrum. For PV devices that support PEC structures in a monolithic device, however, the role of the PV supporting structure is to overcome the water-splitting overpotentials while

* Corresponding author. Tel.: +31 015 27 88903.
E-mail address: r.a.vasudevan@tudelft.nl (R. Vasudevan).

http://dx.doi.org/10.1016/j.solmat.2016.02.006
0927-0248/

driving the necessary current to maximize the STH efficiency that the photoactive electrode is capable of. Another way of saying this is that the *J–V* curve of the PV device under the transmitted light spectrum of the PEC junction should intersect the saturation current of the PEC. In this work, an alternative PV structure is proposed for the a-SiC:H photocathode to realize a silicon based and bias free prototype with a high STH efficiency. This PV component consists of a thin-film, nano-crystalline silicon (nc-Si:H) top cell and a silicon heterojunction (SHJ) bottom cell. A schematic of the monolithic structure with an a-SiC:H photocathode and the supporting nc-Si:H/SHJ stack is given in Fig. 2a. It should be noted that to achieve a monolithic support structure, the solar cell should be illuminated from the n-side rather than traditional p-side illumination for nc-Si:H and SHJ technology. For the SHJ cell, in particular, this resulted in a decision to use a p-type wafer instead of the traditional n-type wafer. Though state of the art SHJ solar cells based on n-type wafers can achieve efficiencies of up to 25.6%, [14] progress has also been made on p-type c-Si wafers [15,16]. A cross-sectional scanning electron microscope (SEM) image of the hybrid cell highlighting the high quality nc-Si:H junction is shown in Fig. 2b.

Nc-Si:H and SHJ technologies were chosen as they can properly utilize the transmitted spectrum of a-SiC:H as shown in Fig. 2c. This transmitted spectrum was measured with the same class AAA solar simulator that is used for *J–V* measurements in this work. Having two PV cells with bandgaps of 1.1 eV is a very effective way to utilize the remaining spectrum shown in red in Fig. 2c. This work shows the optimization of this hybrid nc-Si:H/SHJ solar cell as a component in the silicon based PEC/PV device as well as a simulation of how the hybrid cell will perform in the full PEC/PV monolithic device along with an a-SiC:H photocathode.

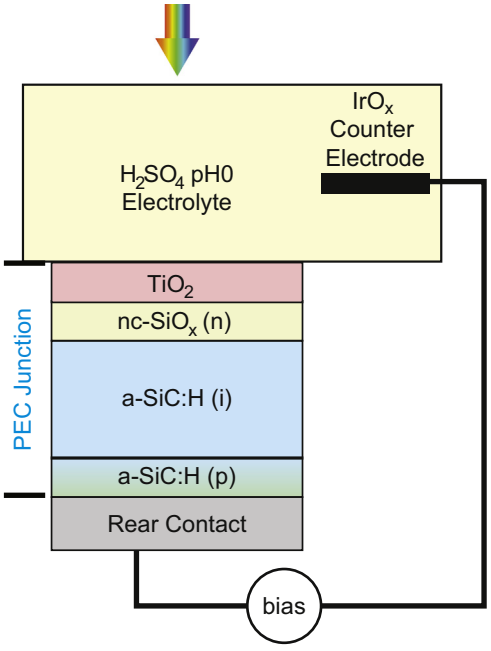

Fig. 1. Schematic illustration of an a-SiC:H photocathode. Note a 1 nm platinum catalyst is not present in the sketch.

2. Experimental setup

2.1. Photocathode preparation

In this work, an a-SiC:H photocathode was fabricated to determine the design rules for the supporting PV structure. The details of its fabrication by radio-frequency plasma-enhanced chemical vapor deposition (RF-PECVD) are shown elsewhere [8]. It was deposited on a corning glass substrate. The photocathode stack consisted of a 10 nm p-doped a-SiC:H(B) layer, a 40 nm gradient p-doped a-SiC:H(B) layer, a 100 nm intrinsic a-SiC:H layer, a 10 nm nc-SiO_x layer with a 25 nm TiO_2 layer coated with a 1 nm platinum catalyst. The individual layers that make up the PEC were independently deposited and measured with spectroscopic ellipsometry (SE) to obtain their optical parameters for use in optical simulations.

The *J–V* of the a-SiC:H photocathode was measured under simulated AM 1.5 solar illumination (100 mW cm^{-2}) using a NEWPORT Sol3A Class AAA solar simulator (type 94023A-SR3). A spot of 6 mm in diameter on the photocathode was illuminated, corresponding to an active area of 0.283 cm^2. A plated iridium oxide (IrO_x) counter-electrode was utilized. An electrolyte with a

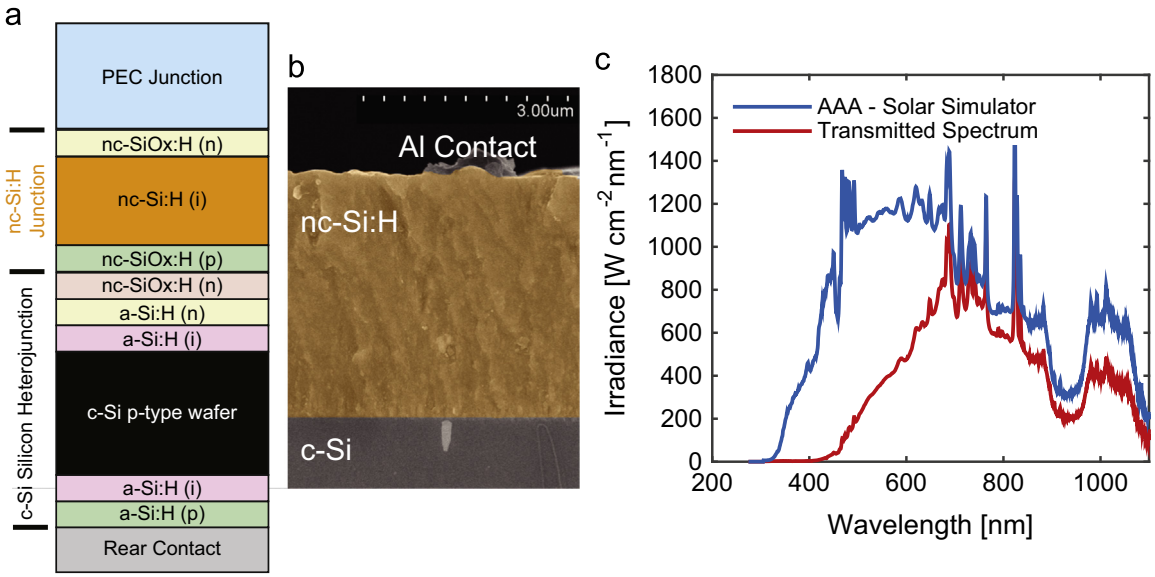

Fig. 2. (a) Schematic illustration of the monolithic PEC/PV cathode based on a-SC:H/nc-Si:H/SHJ structure. (b) SEM cross section of the standalone PV hybrid cell. (c) Measurement of solar simulator spectrum as well as the transmitted spectrum after the a-SiC:H photocathode. (For interpretation of the references to color in this figure caption, the reader is referred to the web version of this paper.)

1 M concentration of sulfuric acid (H_2SO_4) with a pH of 0 is used. These measurements show how the photocathode acts in a complete PEC cell as a two-electrode measurement was used. Therefore, barriers in the whole water-splitting system, such as losses in the counter electrode and properties of the electrolyte, are all considered [17,18].

2.2. Optical simulations

Optical simulations were carried out using an in-house built software GenPro. GenPro uses a 1D simulation tool to solve Fresnel equations and determine how much light is absorbed in the absorber layer of each junction. This absorption amount is converted to an incident photon conversion efficiency (IPCE) for the case of the PEC junction and an external quantum efficiency (EQE) in the case of PV junctions. The electrical losses are neglected here as this is only the first approximation. In the case of the c-Si wafer, optical data from Green et al. was used [19]. In the case of nc-Si, optical data from Murata et al. was used [20]. For the other thin-film layers, SE data was used to extract the relevant optical parameters for the simulation. These simulations served to determine optimal thicknesses to current match the absorber materials in the a-SiC:H/nc-Si:H/SHJ PEC/PV device as well as the standalone nc-Si:H/SHJ hybrid PV cell produced in this work.

2.3. Solar cell fabrication

The fabrication of the SHJ and nc-Si:H were carried out using the same PECVD clustertools. For the SHJ solar cells, ~280 μm thick, ~4.0 in in diameter, double-side polished float-zone c-Si ⟨100⟩ oriented wafers from Topsil were used as substrates. These substrates were cleaned according to a standard procedure described elsewhere [21]. The final termination step was carried out in a 0.5% diluted HF solution for 40 s. The a-Si:H layers were prepared using RF-PECVD and Indium Tin Oxide (ITO) was deposited using a magnetron sputtering tool. Contacts were deposited using physical vapor deposition (PVD).

The nc-Si:H single-junction solar cells were prepared on a piece of flat Corning XG glass as growth on this substrate would closely resemble growth on a flat wafer used in the hybrid tandem device. Indium Tin Oxide (ITO) was deposited on the glass using a magnetron sputtering tool. This was followed by a protective aluminum doped zinc oxide (AZO) protective layer, which was also deposited using sputtering. The remaining layers were deposited using RF-PECVD. The stack is made up of doped nanocrystalline silicon oxide layers (nc-SiO_x:H) and an intrinsic nc-Si:H layer. The deposition conditions have been explained elsewhere [22].

2.4. Solar cell characterization

The *J–V* characteristics of all solar cells were measured under illumination of a WACOM Class AAA solar simulator. External quantum efficiency (EQE) measurements were performed with an in-house setup, utilizing a monochromatic light source. The *J–V* curves presented here have been transposed using the current density values measured by EQE in order to avoid overestimation from the *J–V* measurements. For the transmitted spectrum *J–V* measurement in Fig. 7c, the full a-SiC:H device was used as a light filter resulting in the red spectrum as shown in Fig. 2c.

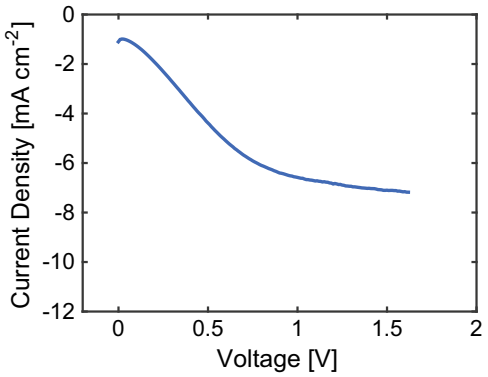

Fig. 3. The *J–V* curve of an a-SiC:H photocathode as measured with a two-electrode measurement with an IrO_x counter electrode.

3. Results

3.1. Photocathode

Fig. 3 shows the performance of the a-SiC:H PEC device without a supporting solar cell. At 0 V external bias, this PEC cell only produces around 1 mA cm^{-2} though significant curents up to 6.5 mA cm^{-2} are possible with an external bias. This *J–V* curve provides us with the parameters necessary for designing a supporting PV structure. Based on the *J–V* curve in Fig. 3, the PV cell should be able to deliver a current density of 6–7 mA cm^{-2} at a voltage of 0.8–1.0 V. This should be achieved under the illumination of the transmitted spectrum through the a-SiC:H layers as shown in Fig. 2c. Enhancements in photocathode technology will eventually increase the current density produced here shifting the *J–V* curve downwards to an eventual saturation current of up to 19.7 mA cm^{-2} [23]. Enhancements in catalyst and counter-electrode technology will also reduce the overvoltage of the PEC system shifting the curve to the left. Therefore producing a hybrid cell that can produce higher currents at around 0.8–1.0 V is favorable taking into account these future enhancements.

3.2. Simulations

Before implementing this solar cell, simulations were carried out to determine the optimum thickness of the nc-Si:H absorber layer. Fig. 4 shows the absorption spectrum of the a-SiC:H (PEC), nc-Si:H (PV) and SHJ (PV) cells, whereas Fig. 5 shows the optimized simulation of a nc-Si:H/SHJ hybrid tandem cell illuminated by simulated AM 1.5 solar spectrum.

For a first approximation, the thickness of the c-Si wafer was held constant as 280 μm and the thicknesses of the PEC and nc-Si:H junction were changed until ideal current matching conditions. In this case, current matching occurred with an a-SiC:H thickness of 415 nm and a nc-Si:H thickness of 9.2 μm. This resulted in a matched current of 10.7 mA cm^{-2}. The spectral absorption is given in Fig. 4a. These thicknesses are unrealistic as devices with those thicknesses would exhibit significant electrical losses and require long deposition times. This does, however, present the maximum current that can be produced if light trapping techniques are utilized to maximize the optical thickness of the thin film absorber layers while leaving them realistically thin.

Another simulation was carried out with a limit of 5 μm applied to the nc-Si:H absorber layer. Here an a-SiC:H thickness of 246 nm produces the highest current of 9.4 mA cm^{-2} even though the SHJ will produce a higher current of 12.9 mA cm^{-2}. The spectral absorption of this, more realistic option, is given in Fig. 4b.

As the focus of this paper is the optimization of the nc-Si:H/SHJ PV stack, simulations were also carried out to current match the

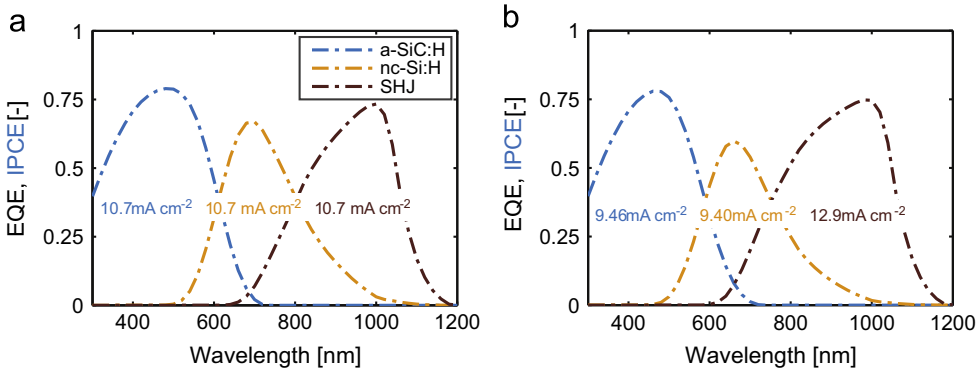

Fig. 4. Simulated IPCE of an a-SiC:H photocathode and EQE of supporting PV stack. (a) Thicknesses used to achieve ideal current matching. (b) Practical thicknesses used.

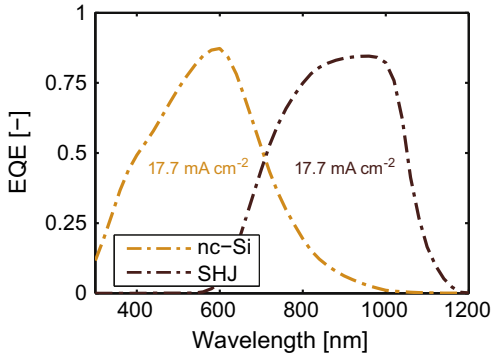

Fig. 5. Optical simulation of standalone nc-Si/SHJ PV stack.

Table 1
External parameters of single junction n-illuminated nc-Si:H solar cell on textured substrate as well as on flat substrate with n-side illumination.

Parameter	Optimal device [22]	Flat substrate w/ n-illumination
Thickness (μm)	3	2.5
V_{OC} (V)	0.551	0.532
J_{SC} (mA cm^{-2})	26.0	20.04
FF	0.701	0.694
η (%)	10.0	7.40

PV junction with a full AM 1.5 spectrum. Fig. 5 shows the EQE of a thickness optimized double-junction cell that ignores the photocathode. As shown here, a thickness of 2.8 μm in the nc-Si:H absorber gives a very closely matched current of 17.7 mA cm^{-2} with the wafer of the SHJ. Though the ideal layer thickness for a current matched double cell is predicted here to be 2.8 μm, 3.5 μm was used as this would serve to perform better in the transmitted spectrum used to simulate using this PV stack in a monolithic device while still achieving comparable currents in AM 1.5 conditions.

3.3. Single junction solar cells

The hybrid tandem cell required the development of nc-Si:H solar cells and SHJ solar cells that are illuminated from the n-side. This section presents the challenges involved in engineering both of these single junctions as solar cells illuminated from n-side.

In the case of nc-Si:H, efficiencies of above 10% have been reported with these deposition conditions [22]. However, this was based on a growth on a textured substrate with p-side illumination. Table 1 shows the external parameters of the solar cell when deposited on a flat substrate and illumination from the n-side as compared to the best results reported with this recipe. It should be noted that these devices cannot be directly compared due to a difference in the thickness of the absorber layer. However, due to the poorer light trapping properties of a flat device and the electrical and shading losses from the n-side illumination, J_{SC} decrease significantly. The V_{OC} and *FF* do not deviate significantly from the textured, p-side illuminated cell.

For the SHJ, a p-type ⟨100⟩ wafer was used. It should be noted that a rear emitter solar cell with a n-type wafer is also possible, though better results were obtained here by using a p-type wafer. One parameter that was important for improving the efficiency of this junction in the cell stack was the front i-layer. Wei et al. have shown that increasing the thickness of the front i-layer on a p-type SHJ solar cell increases the J_{SC} and *FF* [24]. Repeating this experiment showed similar results as shown in Fig. 6. The J_{SC} is the main factor for the increase in STE efficiency here. The increase in J_{SC} points to a current collection issue at the front n/i interface when the i-layer is not of a sufficient thickness.

3.4. Hybrid Tandem Solar Cell

The black, dashed line in Fig. 7a shows the *J–V* curve of the first hybrid tandem cell. A thickness of 3.5 μm was used for the nc-Si:H intrinsic, absorber layer. There is a notable S curve indicating a large barrier in the solar cell. Engineering the tunneling recombination junction (TRJ) mitigates this. Two main approaches for this optimization were carried out. The first approach was to add a n-type nc-SiO_x layer between the two junctions. A discussion of the processing techniques of this material is presented elsewhere [25]. This was followed by an increase in the doping of the n-layer of the SHJ by increasing the phosphine flow in the processing plasma. Fig. 7a shows how engineering the TRJ effects the *J–V* curve of the solar cell and it is evident that adding nc-SiO_x and increasing the doping of the SHJ n-layer significantly improves the performance of the PV cell. The resultant nc-Si:H/SHJ hybrid tandem cell has a V_{OC} of 1.1 V and an efficiency, under AM 1.5 illumination, of 10.3%.

This is consistent with engineering of multijunction thin-film silicon devices such as so-called micromorph solar cells. N-type nc-SiO_x has been used in TRJs of micromorph cells to improve both optical and electrical characteristics [26]. Adding highly doped layers at the TRJ has increased recombination in this junction and thus improved multijunction solar cell efficiencies [27]. Having a relatively lower doped TRJ creates a barrier in the tandem device whereas adding highly doped layers in the TRJ increases recombination, which aids in the performance of multijunction devices and shows here to be essential when engineering a nc-Si:H/SHJ tandem device.

Fig. 7b shows an EQE of this solar cell. This demonstrates that current matching under AM 1.5 illumination conditions was achieved. The two junctions of this hybrid cell achieve a spectral

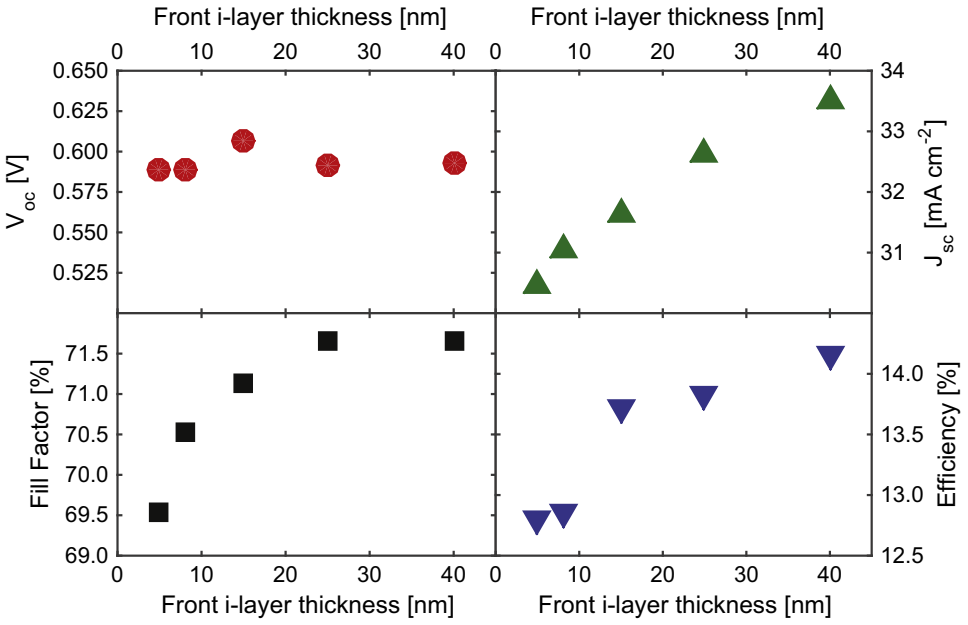

Fig. 6. External parameters of SHJ solar cells based on a p-type wafer from varying the thickness of the i-layer on the emitter side.

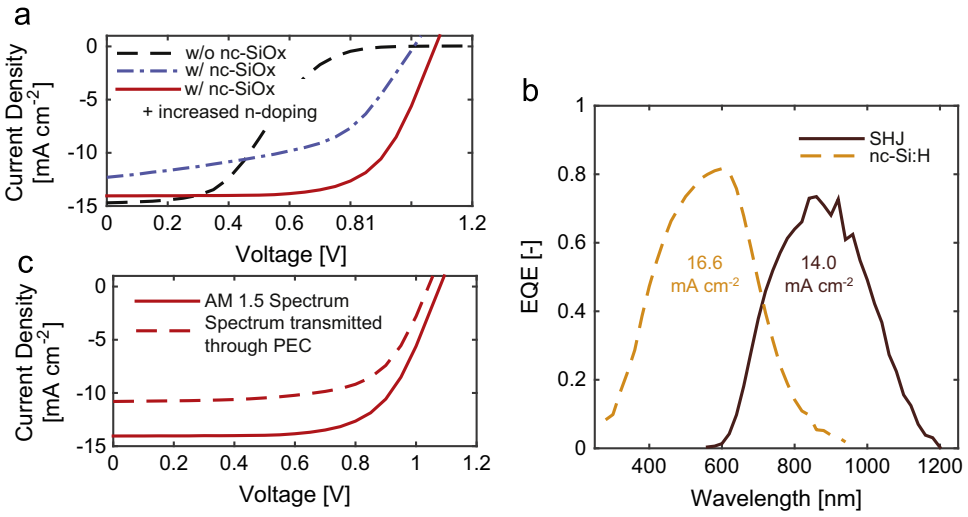

Fig. 7. Optimization of nc-Si:H/SHJ hybrid tandem cell. (a) *J–V* curve of the hybrid solar cell with different TRJ configurations. (b) EQE curves of the optimized hybrid solar cell. (c) Shifting of the *J–V* curve of the hybrid cell when a standard PEC is used as a filter to only allow the light that would hit the hybrid cell if it were integrated into a monolithic PEC/PV structure.

utilization of 30.6 mA cm^{-2} with a flat configuration. Though this works as a first step into thin-film silicon/SHJ hybrid tandem cell technologies for water splitting, implementing light trapping techniques such as texturing and intermediate reflectors with this technology could achieve a greatly improved spectral utilization. Further optimization of the TRJ and better performing p-type SHJ solar cells (V_{OC} of 0.717 V have been reported [15]) could potentially increase the V_{OC} of this hybrid device to between 1.2 and 1.3 V.

4. Integration simulation

In order to determine the potential of this hybrid tandem cell in the PEC/PV hybrid tandem structure for water splitting, the performance of the solar cell under the spectrum transmitted by the a-SiC:H photocathode must be produced. This transmitted spectrum is shown in Fig. 2b. The spectrum was produced by taking an a-SiC:H photocathode and using it as an optical filter under the WACOM solar simulator in front of the nc-Si:H/SHJ hybrid tandem device. The resulting *J–V* curve is shown in Fig. 7c. It is clear that the operating points are reduced because of the more limited illumination conditions.

This *J–V* curve can be overlaid with the measured spectra of the a-SiC:H photocathode, which has been shown in Fig. 3b. The overlapping *J–V* curves are given in Fig. 8. The crossing point of this graph predicts that if the nc-Si:H/SHJ hybrid cell were to be used as a supporting solar cell structure, it would produce a current density of 6.43 mA cm^{-2} which corresponds to an STH efficiency of 7.90%. Improvements in PEC technology will shift the *J–V* curve of the PEC down and to the left pushing the ideal crossing point closer to the maximum power point of the hybrid PV cell presented here. Therefore as PEC technology progresses, the hybrid cell will be an even more suitable candidate for a PV support structure.

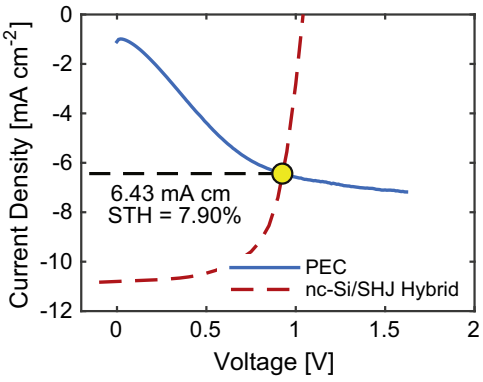

Fig. 8. Integration simulation of nc-Si:H/SHJ hybrid tandem cell with a-SiC:H based photocathode. *J–V* curve of hybrid PV structure and PEC curve shown along with predicted current density and STH efficiency.

5. Conclusions

This paper has demonstrated the capabilities of using an a-SiC:H photocathode with a nc-Si:H/SHJ hybrid solar cell as a supporting structure. A working solar cell has been produced yielding a STE efficiency of 10.4% under an AM 1.5 spectrum. Tunneling recombination engineering has been identified and addressed as an important consideration for this hybrid device where the use of nc-SiO_x and doping concentrations of the SHJ n-layer can significantly improve the efficiency of the solar cell. Furthermore, an integration of the solar cell with current PEC technology has been simulated predicting a high operating current of 6.43 mA cm^{-2} corresponding to a STH efficiency of 7.90%.

Acknowledgments

The authors of this paper would like to acknowledge the technicians Martijn Tijssen, Stefaan Heirman and Remko Koornneef without whom this work would not be possible. This work was funded by STW under the Fundamentals and Applications of Silicon Heterojunctions (FLASH) under the Project code 12166.

Appendix A. Supplementary data

Supplementary data associated with this paper can be found in the online version at http://dx.doi.org/10.1016/j.solmat.2016.02.006.

References

[1] O. Khaselev, A Monolithic Photovoltaic-Photoelectrochemical Device for Hydrogen Production via Water Splitting, 1998. http://dx.doi.org/10.1126/science.280.5362.425.
[2] S. Licht, Multiple band gap semiconductor/electrolyte solar energy conversion, J. Phys. Chem. B 105 (3) (2001) 6281–6294, http://dx.doi.org/10.1021/jp010552j.
[3] J. Hu, F. Zhu, I. Matulionis, A. Kunrath, T. Deutsch, E. Miller, A. Madan, Solar-to-hydrogen photovoltaic/photoelectrochemical devices using amorphous silicon carbide as the photoelectrode, in: 23rd European Photovoltaic Solar Energy Conference, 2008.
[4] F. Zhu, J. Hu, A. Kunrath, I. Matulionis, B. Marsen, B. Cole, E. Miller, A. Madan, a-SiC:H films used as photoelectrodes in a hybrid, thin-film silicon photoelectrochemical (PEC) cell for progress toward 10% solar-to hydrogen efficiency, Solar Hydrog. Nanotechnol. II 6650 (2007) 66500S–66500S-9. http://dx.doi.org/10.1117/12.735014.
[5] F. Zhu, J. Hu, I. Matulionis, T. Deutsch, N. Gaillard, A. Kunrath, E. Miller, A. Madan, Amorphous silicon carbide photoelectrode for hydrogen production directly from water using sunlight, Philos. Mag. 89 (28–30) (2009) 2723–2739, http://dx.doi.org/10.1080/14786430902740729.
[6] I.A. Digdaya, L. Han, T. Buijs, M. Zeman, B. Dam, A.H.M. Smets, W.A. Smith, Extracting Large photovoltages from a-SiC Photocathodes with an amorphous TiO_2 front surface field layer for solar hydrogen evolution, Energy Environ. Sci. 8 (2015) 1585–1593, http://dx.doi.org/10.1039/C5EE00769K.
[7] S. Hu, C. Xiang, S. Haussener, A.D. Berger, N.S. Lewis, An analysis of the optimal band gaps of light absorbers in integrated tandem photoelectrochemical water-splitting systems, Energy Environ. Sci. 6 (4) (2013) 2984, http://dx.doi.org/10.1039/c3ee40453f.
[8] L. Han, I.A. Digdaya, T.W. Buijs, F. Abdi, Z. Huang, R. Liu, B. Dam, M. Zeman, W. A. Smith, A.H.M. Smets, Gradient dopant profiling and spectral utilization of monolithic thin-film silicon photoelectrochemical tandem devices for solar water splitting, J. Mater. Chem. A (2014) 1–8, http://dx.doi.org/10.1039/C4TA05523C.
[9] J.R. Bolton, S.J. Strickler, J.S. Connolly, Limiting and realizable efficiencies of solar photolysis of water, Nature 316 (6028) (1985) 495–500, http://dx.doi.org/10.1038/316495a0.
[10] M.F. Weber, Efficiency of splitting water with semiconducting photoelectrodes, J. Electrochem. Soc. 131 (6) (1984) 1258, http://dx.doi.org/10.1149/1.2115797.
[11] A. Stavrides, A. Kunrath, J. Hu, R. Treglio, A. Feldman, B. Marsen, B. Cole, E. Miller, A. Madan, Use of amorphous silicon tandem junction solar cells for hydrogen production in a photoelectrochemical cell, SPIE 6340 (2006) 1–8, http://dx.doi.org/10.1117/12.678870.
[12] L. Han, F.F. Abdi, P. Perez Rodriguez, B. Dam, R. van de Krol, M. Zeman, A.H. M. Smets, Optimization of amorphous silicon double junction solar cells for an efficient photoelectrochemical water splitting device based on a bismuth vanadate photoanode, Phys. Chem. Chem. Phys. 16 (9) (2014) 4220, http://dx.doi.org/10.1039/c3cp55035d.
[13] F.F. Abdi, L. Han, A.H.M. Smets, M. Zeman, B. Dam, R. van de Krol, Efficient solar water splitting by enhanced charge separation in a bismuth vanadate-silicon tandem photoelectrode, Nat. Commun. 4 (2013) 2195, http://dx.doi.org/10.1038/ncomms3195.
[14] M.A. Green, K. Emery, Y. Hishikawa, W. Warta, E.D. Dunlop, Solar cell efficiency tables (version 44), Prog. Photovolt.: Res. Appl. 22 (2014) 701–710, http://dx.doi.org/10.1002/pip.2525.
[15] A. Descoeudres, Z.C. Holman, L. Barraud, S. Morel, S. De Wolf, C. Ballif, 21% efficient silicon heterojunction solar cells on n- and p-type wafers compared, IEEE J. Photovolt. 3 (1) (2013) 83–89, http://dx.doi.org/10.1109/JPHOTOV.2012.2209407.
[16] S. De Wolf, A. Descoeudres, Z.C. Holman, C. Ballif, High-efficiency silicon heterojunction solar cells: a review, Green 2 (1) (2012) 7–24, http://dx.doi.org/10.1515/green-2011-0018.
[17] R. van de Krol, M. Grätzel, Photoelectrochemical Hydrogen Production, 2012. http://dx.doi.org/10.1007/978-1-4614-1380-6.
[18] C. Zoski, Handbook of Electrochemistry, 2007.
[19] M.A. Green, Self-consistent optical parameters of intrinsic silicon at 300 K including temperature coefficients, Solar Energy Mater. Solar Cells 92 (11) (2008) 1305–1310, http://dx.doi.org/10.1016/j.solmat.2008.06.009.
[20] D. Murata, T. Yuguchi, H. Fujiwara, Characterization of μc-Si:H/a-Si:H tandem solar cell structures by spectroscopic ellipsometry, Thin Solid Films 571 (2013) 756–761, http://dx.doi.org/10.1016/j.tsf.2013.10.073.
[21] D. Zhang, I. Digdaya, R. Santbergen, R. van Swaaij, P. Bronsveld, M. Zeman, J. van Roosmalen, A.W. Weeber, Design and fabrication of a SiOx/ITO double-layer anti-reflective coating for heterojunction silicon solar cells, Solar Energy Mater. Solar Cells 117 (2013) 132–138, http://dx.doi.org/10.1016/j.solmat.2013.05.044.
[22] H. Tan, E. Psomadaki, O. Isabella, M. Fischer, P. Babal, R. Vasudevan, M. Zeman, A.H.M. Smets, Micro-textures for efficient light trapping and improved electrical performance in thin-film nanocrystalline silicon solar cells, Appl. Phys. Lett. 103 (17) (2013) 173905, http://dx.doi.org/10.1063/1.4826639.
[23] C.-H. Cheng, J.-H. Chang, C.-I. Wu, G.-R. Lin, Semi-transparent silicon-rich silicon carbide photovoltaic solar cells, RSC Adv. 5 (46) (2015) 36262–36269, http://dx.doi.org/10.1039/C4RA16998K.
[24] C.-Y. Wei, C.-H. Lin, H.-T. Hsiao, P.-C. Yang, C.-M. Wang, Y.-C. Pan, Efficiency improvement of HIT solar cells on p-type Si wafers, Materials 6 (11) (2013) 5440–5446, http://dx.doi.org/10.3390/ma6115440.
[25] P. Babal, J. Blanker, R. Vasudevan, A.H.M. Smets, M. Zeman, Microstructure analysis of n-doped μc-SiOx:H reflector layers and their implementation in stable a-Si:H p-i-n junctions, in: Conference Record of the IEEE Photovoltaic Specialists Conference, 2012, pp. 321–326. http://dx.doi.org/10.1109/PVSC.2012.6317627.
[26] P.D. Veneri, L.V. Mercaldo, I. Usatii, Improved micromorph solar cells by means of mixed-phase n-doped silicon oxide layers, Prog. Photovolt.: Res. Appl. 20 (2012) 148–155, http://dx.doi.org/10.1002/pip.
[27] S.S. Hegedus, F. Kampas, J. Xi, Current transport in amorphous silicon np junctions and their application as “tunnel” junctions in tandem solar cells, Appl. Phys. Lett. 67 (1995) (1995) 813, http://dx.doi.org/10.1063/1.115452.